PAN

MODEL RESEARCH OF GAS EMISSIONS FROM LIGNITE AND BIOMASS CO-COMBUSTION IN A LARGE SCALE CFB BOILER

Jarosław Krzywański[1], Rafał Rajczyk[*1], Wojciech Nowak[2]

[1]Czestochowa University of Technology, Institute of Advanced Energy Technologies, Dąbrowskiego 73, 42-201 Czestochowa, Poland

[2]AGH University of Science and Technology, Krakow, Poland

The paper is focused on the idea of a combustion modelling of a large-scale circulating fluidised bed boiler (CFB) during coal and biomass co-combustion. Numerical computation results for three solid biomass fuels co-combustion with lignite are presented in the paper. The results of the calculation showed that in previously established kinetics equations for coal combustion, some reactions had to be modified as the combustion conditions changed with the fuel blend composition. Obtained CO_2, CO, SO_2 and NO_x emissions are located in borders of $\pm 20\%$ in the relationship to the experimental data. Experimental data was obtained for forest biomass, sunflower husk, willow and lignite co-combustion tests carried out on the atmospheric 261 MWe COMPACT CFB boiler operated in PGE Turow Power Station in Poland. The energy fraction of biomass in fuel blend was: $7\%_{wt}$, $10\%_{wt}$ and $15\%_{wt}$. The measured emissions of CO, SO_2 and NO_x (i.e. $NO + NO_2$) were also shown in the paper. For all types of biomass added to the fuel blends the emission of the gaseous pollutants was lower than that for coal combustion.

Keywords: biomass; circulating fluidised bed; co-combustion; lignite; modelling

1. INTRODUCTION

Coal and biomass co-combustion is one of the ways to meet the requirements for reduction of gaseous pollutant emissions. As biomass material is considered to be a renewable source of energy it is used as a fuel in power boilers. Biomass co-combustion in a CFB boiler takes the advantage of fluidised bed fuel flexibility. Biomass material differs from coal with respect to many characteristics; Jenkins et al. (1998), Werther (2009). Different from coal chemical constitution of biomass affects co-combustion processes and makes them more complex. There are many papers dealing with coal and biomass co-combustion: Abelha et al. (2002), Armesto et al. (2003), Armesto et al. (2008), Bahillo et al. (2003), Hein and Bemtgen (1998), Hupa (2005), Gayan et al. (2004), Jenkins et al. (1998), Knobig et al. (1998), Leckner (2004), Leckner (2007), Leckner (2008), Liu and Gibbs (2002), Lyngfelt and Leckner (1999), McIlveen-Wright et al. (2006), Nussbaumer (2003), Sami et al. (2001), Skreiberg et al. (2004), Thunman et al. (2002), Werther (2009), Yu et al. (2009). Co-firing tests in a CFB boiler of olive cake, straw pellets, meat and bone meal and wood pellets mixed with bituminous Colombian coal in the proportions of 5, 15 and 25% of biomass by weight were presented by Abelha et al. (2008). The authors noticed that combustion of biomass material takes place mainly in the combustion chamber, leading to the temperature increase in the upper part in comparison to the dense bed zone. A decrease of CO emissions was also observed with the biofuel fraction for all types of biomass and two reasons were given for that: an increase of the secondary air supply, resulting from higher volatile matter and

---

*Corresponding author, e-mail: rafalr@is.pcz.czest.pl

improved mixing in the combustion chamber, and an increase of temperature in the riser caused by biofuel volatile combustion.

Lower NO_x emissions were also observed for all types of biomass, even though meat and bone meal had six times more nitrogen than coal. As the explanation the authors underlined the role of $deNO_x$ mechanism, favoured by the presence of H and OH radicals from volatiles. According to this mechanism, NH_3- the main product of thermal decomposition of amino acid structures, released in the combustion chamber, reacts with NO_x forming N_2. SO_2 emissions decreased with the increase of biofuel fraction mainly due to lower S content for all types of biomass except that for coal.

A strong dependency of the flue gas composition on the sort of combusted fuel is discussed by Hupa (2005). The author stated that there are no sufficient data on the behavior of fuels when they are burned in various mixtures. Describing results of wood and bituminous coal co-combustion tests, performed by Chalmers University of Technology in Sweden at the 12 MW circulating fluidised bed boiler the author noticed that sulphur dioxide emissions were a linear function of the fuel composition and increased with the bituminous coal share in the blend of fuels. Similar observation were made by Leckner (2007). Hupa (2005) who concluded, that generally all of SO_2 originates in the coal as the alkaline ash in the wood is known to be able to capture SO_2 released during wood combustion.

NO emissions were roughly the same for pure fuels, i.e. coal and wood, in spite of the fact that nitrogen content in wood was about 10 times smaller than that for coal. As it was explained, NO in the lower part of the fluidised bed, formed during wood combustion, remains roughly the same along the rest of the combustion chamber as the bed contains less char than that during coal combustion (Hupa, 2005). Similar observations were presented by Leckner (2007), where the author pointed out the peculiar shape of the curve describing NO emissions. The emission of NO during combustion of wood alone was somewhat higher than that from coal combustion. The concentrations of nitrogen oxides first increased with the increase of coal fraction in fuel blend and then decreased. The author explained it by the difference between char content in coal and in wood since char has the capability to reduce NO concentration (Leckner, 2007). A similar observation was made for CO emissions. The reason for that was the nature of volatile combustion, which takes place in the upper part of the combustion chamber, even in the cyclone, as biomass material contains more volatile matters than coal, thus leading to an increase of temperature and enhancing burnout in this part of the combustion chamber (Leckner, 2007).

Different ways in which co-combustion can be organised highlighting the advantages of CFB boilers are discussed by Leckner (2008). The co-firing results of sewage sludge with coal and wood under CFB conditions were described by Leckner et al. (2004). Investigations were carried out in a laboratory-scale plant and a pilot scale 12MWth CFB boiler. The authors confirmed a dominant role of char in NO and N_2O reduction. A review of combustion and co-combustion of biomass technologies is also given by Nussbaumer (2003). A decrease in SO_x and NO_x concentration was noticed when co-firing biomass and coal in fluidised beds, due to lower sulphur and nitrogen content in biomass. The author noted, that a high volatile content of biomass fuels favours NO_x reduction. Sami et al. (2001) emphasised the previously mentioned $DeNO_x$ mechanism in NO_x reduction. No increase of gaseous pollutant emission was also observed by Hein and Bemtgen (1998). The authors described the results of several co-combustion studies performed under the EU-project "Combined Combustion of Biomass/Sewage Sludge and Coals of High and Low Rank in Different Systems of Semi-industrial and Industrial Scale". Some of them were conducted using CFB facilities: 0.3 MW_{th} INETI, 1 MW_{th} CIEMAT, 1 MW_{th} RWE Energie and 80 MW_{th} CFB at Grenaa, ELSAM/Midtkraft. All partners involved in the project confirmed that biomass co-combustion leads to SO_2 reduction. Low NO_x emissions were also observed in some cases roughly at the same biomass addition. Others found that NO_x concentrations decreased in flue gas during co-combustion, due to lower fuel-N content in biomass (Hein and Bemtgen, 1998).

Co-combustion of pine bark with lignite and bituminous coal in the CIEMAT 0.3 MW_{th} CFB boiler was described by Bahillo et al. (2003). With the increased amount of pine bark in the fuel blend the

temperature in the top of the riser increased. The emissions of CO and SO_2 decreased with the biomass fraction in the fuel blend. The authors noted that higher volatile content and thus higher reactivity of biomass fuels results in a rapid burn-out and lower CO concentrations. Lower S content in the biomass leads to lower SO_2 emissions. They also observed a decrease of NO_x emissions with a share of pine bark in the fuel mixture with bituminous coal due to fast release of volatile matter from biomass causing high levels of hydrocarbon radicals (Bahillo et al., 2003).

Armesto et. al. (2002) investigated the influence of temperature and fluidisation velocity on the combustion efficiency and CO emissions during rice husk combustion in a 30 kWth atmospheric bubbling fluidised bed pilot plant of CIEMAT. Combustion efficiency was higher than 97%. It was also shown that CO emissions strongly depend on the temperature profile in the furnace.

The CIEMAT fluidised bed pilot plant was also used for co-firing of lignite and anthracite with a biomass waste from the olive oil industry - foot cake (Armesto et al., 2003). The fuel-N conversion to NO_x increased with the rank of coal. A slight decrease of NO_x emissions was noticed during co-combustion due to higher volatile matter content in biomass. An interesting chemical kinetic model for the oxidation of ammonia was presented by Skreiberg et al. (2004). The authors pointed out that the model is recommended for modelling of NO reduction by primary measures during combustion of biomass. The technical and economic aspects of coal co-combustion with biomass and plastic wastes in CFB boilers were examined by McIlveen-Wright et al. (2006). Their results show that fluidised bed technology is a very suitable method for co-firing such fuels. The authors noted that co-firing had an almost negligible effect on system efficiency.

Knobig et al. (1998) used wood, peat and coal to investigate the scale-up issue during combustion in a lab-scale facility and 12 MWth boiler, with respect to emissions of flue gas species. The authors determined the axial concentration profiles of oxygen, carbon monoxide, nitric oxide, nitrous oxide and ammonia along the riser height, which were similar both in a small-scale and a large-scale CFB boilers. Nitrous and carbon oxides were rapidly formed to high concentrations in the bottom part of the combustion chamber and then reduced along the reactor.

A study on NO and CO emissions during combustion of wood-chips in a 12 MW CFB boiler was published by Lyngfelt and Leckner (1999). The authors highlighted that lowering the air - fuel ratio in the combustor through secondary air addition in the cyclone inlet resulted in a significant NO reduction without enhancing CO emissions.

The literature contains many other interesting models of coal and biomass combustion in CFB boilers.

A model for the combustion of wood particles in fluidised and fixed-bed combustors was also shown by Thunman et al. (2002). The model takes into account the shrinkage of a particle and demonstrates its great influence on devolatilisation time as well as char combustion. The particle was divided into four regions: moist, dry and devolatilising fuel, char residue and ash. A model of coal and wood co-firing, validated on a pilot-scale 0.1 and 0.3 MWth test-rigs was presented by Gayan et al. (2004). The existence of three zones in the riser: bottom, splash and transport zone were taken into account by the model. It describes solid concentration profiles in the splash and transport zones with an exponential decay model, as the splash zone constitute a region with a sharp decay of solid concentration.

A three-dimensional model of coal and biomass co-combustion in a CFB boiler with a capacity of 130 t/h is presented by Yu et al. (2009). The model uses a commercial FLUENT software. A model of NO and N_2O emissions from the biomass-fired circulating fluidised bed combustors was presented by Liu and Gibbs (2002). The authors applied it to predict NO and N_2O emissions from a 12 MW_{th} CFB boiler. Observed N_2O emissions were less than 5 ppmv while the NO emissions increased with the total excess air and fuel-N content.

Finally, a simplified one-dimensional model of coal and biomass co-combustion was shown by Krzywański et al. (2012). The authors proposed equations for the chemical reaction rate coefficients of some reactions which were then used to describe the biomass and lignite co-combustion under CFB conditions.

The aim of this work is to carry out a computational study of gaseous pollutant emissions from co-combustion of lignite with biomass materials in a large-scale 261 MWe CFB boiler. The model presented in this paper takes into account experiences in modelling performed for a 261 MWe (704 t/h) COMPACT CFB boiler operated in PGE GiEK S.A. Dept. Turow Power Plant in Poland, burning both lignite and biomass. The core of the model was based on the previously established and successfully validated coal combustion model which was used for the study of coal combustion in a large-scale 235 MW_e (670 t/h) CFB boiler and 0.1MW_{th} CFB test rig (Muskała et al., 2008; Krzywański et al., 2010a; Krzywański et al., 2010b; Krzywański et al., 2011). Moreover, the procedure combines also the experience in modelling of lignite and biomass co-firing in a circulating fluidised bed (Krzywański et al., 2013). Therefore, the paper is a continuation and development of the earlier works on numerical simulations of CFB boilers. The model presented in the paper constitute a simplifed instance of previously developed model of biomass and coal co-combustion in CFB boilers presented in (Krzywański et al., 2013).

2. EXPERIMENTAL

The experimental work reported here was carried out on the atmospheric 261 MW_e COMPACT CFB boiler operated in PGE GiEK S.A. Dept. Turow Power Plant in Poland. The combustion chamber has the dimensions of cross-section area equal to 21.9×5.2 m in its lower part, immediately above the grid and 21.9×10.1 m at a height of 8.7 m above the grid level. The total height of the combustion chamber is 42 m. The boiler is fitted with two compact separators, as it belongs to the second generation boilers (Werther, 2005). A detailed description of the system can be found elsewhere (Krzywanski et al., 2013). A scheme of the boiler is presented in Fig.1.
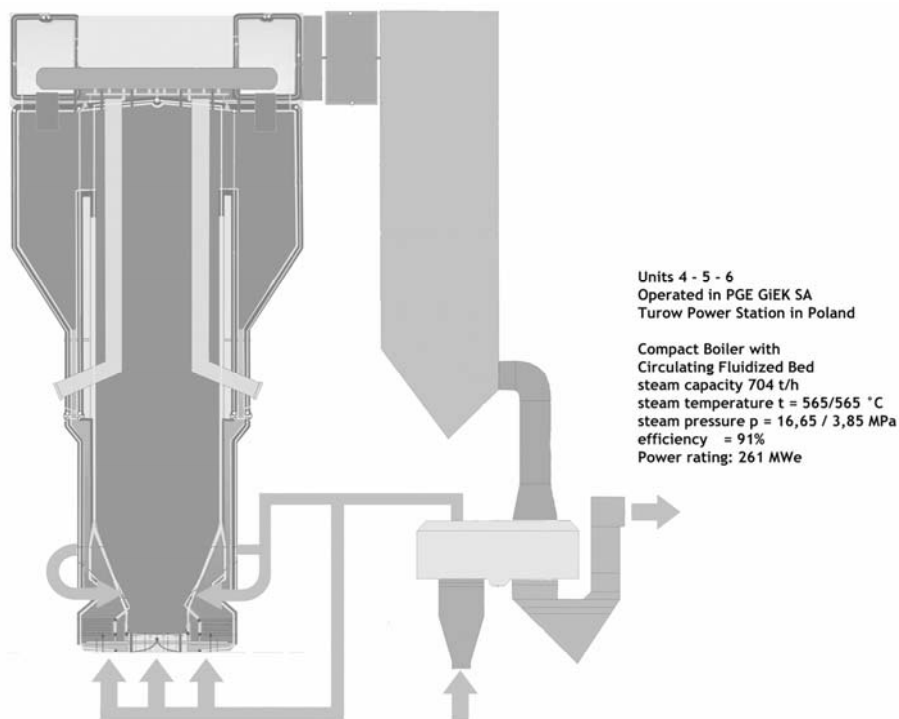

Units 4 - 5 - 6
Operated in PGE GiEK SA
Turow Power Station in Poland

Compact Boiler with
Circulating Fluidized Bed
steam capacity 704 t/h
steam temperature t = 565/565 °C
steam pressure p = 16,65 / 3,85 MPa
efficiency = 91%
Power rating: 261 MWe

Fig. 1. The 261 MW_e COMPACT CFB boiler

The co-firing study was conducted for four tests (tests 1 - 4) involving different shares and types of solid biomass and lignite. Biomass group I (agro & energy crops: sunflower husk, willow) and group II – forest biomass were used in the co-combustion tests. The energy fraction of biomass in fuel blend, fed to the boiler was: 7%, 10% and 15%. An additional test was also performed when only lignite was burned (test 0) to allow a comparative analysis.

Concentrations of the flue gas components, such as: CO_2, CO, SO_2 and NO_x were measured during tests. The gas component measurements (SO_2, H_2O, CO_2, CO, NO_x) were performed using the existing monitoring. The methodology of measurements can be found elsewhere (Krzywanski et al., 2013). Studies were performed for the following fuel mass flows (lignite): test 0 – 55.04 kg/s, test 1- 65.7 kg/s, test 2 – 64.5 kg/s, test 3 – 65.3 kg/s, test 4 – 64.7 kg/s. The fuel mass flow was adjusted to achieve 100 % of the boiler's load. The sorbent mass flows were: test 0 – 4.1 kg/s, test 1 – 3.8 kg/s, test 2 – 4.4 kg/s, test 3 – 3.8 kg/s, test 4 – 4.2 kg/s, Ca/S ratio: 2.8 for test 1 (7% biomass), 3.2 for test 2 (10% biomass), 2.7 for test 3 (15% biomass 1st test), 2.3 for test 4 (15% biomass 2nd test).

The properties and the size distributions of lignite, each type of the biomass and their mixtures, limestone used during co-combustion tests, as well as the operation data of the boiler and other conditions of the experiments are given by Krzywanski et al. (2013). A detailed description of the biomass feeding installation can be found in Rajczyk et al. (2011).

2.1. CO, SO_2 and NO_x emissions

The emissions of CO, SO_2 and NO_x during test 0 coal mono-combustion as well as tests 1-4 of coal and biomass co-combustion are presented in Fig. 2.
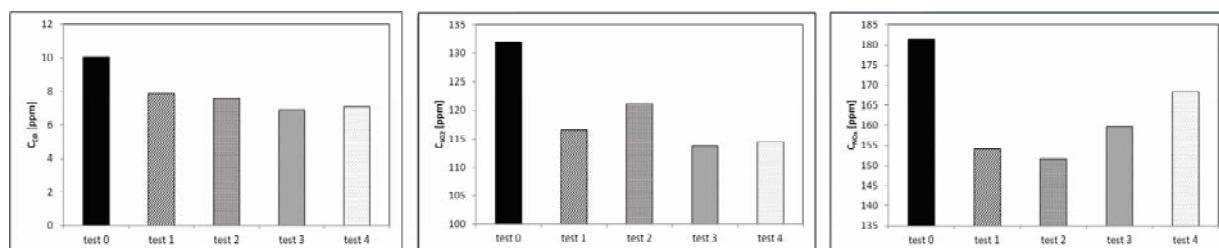

Fig. 2. CO, SO_2, NO_x emissions during combustion and co-combustion tests

A comparison between CO, SO_2 and NO_x emissions observed during biomass co-combustion (tests 1-4) and those obtained during combustion of lignite only (test 0) is shown in Fig. 3.

For all types of biomass included in the fuel blends the gaseous pollutant emissions are lower during co-combustion tests 1- 4 than those for coal mono-combustion test 0. The trends in the CO, SO_2 and NO_x emissions are consistent with results reported in the literature (Abelha et al., 2008; Armesto et al., 2002; Bahillo et al., 2003; Hein and Bemtgen, 1998; Hupa, 2005; Leckner, 2007; Nussbaumer, 2003). The reason for CO reduction could be the nature of volatile combustion, which takes place in the upper part of the combustion chamber. It leads to an increase of temperature in the combustion chamber and enhances the burnout in the upper part of the furnace. The emission of SO_2 decreases due to lower S content in biomass. Similar to the results presented in (Abelha et al., 2008; Armesto et al., 2003; Hein and Bemtgen, 1998; Leckner et al., 2004; Nussbaumer, 2003; Sami et al., 2001) the emissions of NO_x also decreased with a biomass fraction in the fuel blends, even though nitrogen content in biomass was about 3-6 times higher than that in coal. The decrease could be attributed to a higher char content in biomass than that in lignite (Gayan et al., 2004) as char has a capability to reduce NO content. Another explanation could be the $DeNO_x$ mechanism, favoured by the presence of H and OH radicals from volatiles (Hupa, 2005; Sami et al., 2001).
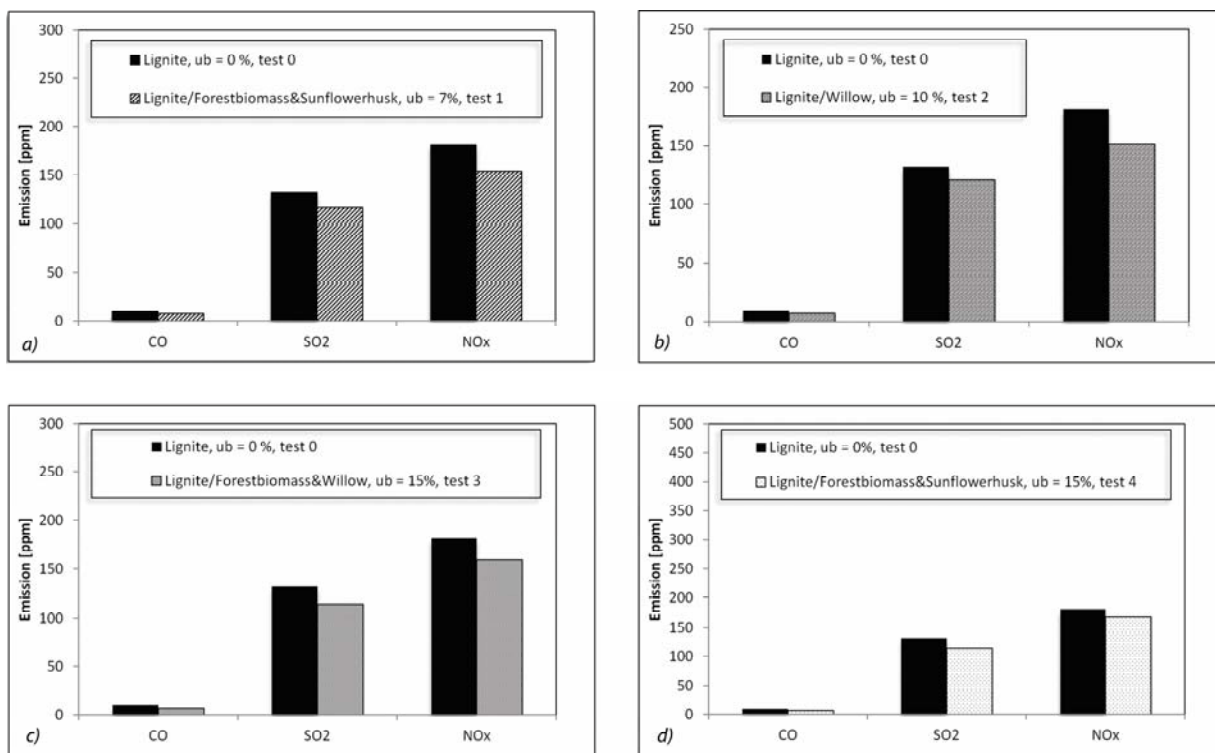
Fig. 3. CO, SO$_2$ and NO$_x$ emissions in combustion test 0 and: a) co-combustion test 1, b) co-combustion test 2, c) co-combustion test 3, d) co-combustion test 4.

2.2. Numerical simulations of CO$_2$, CO, SO$_2$ and NO$_x$ emissions

The model consists of several sub-models enabling to describe crucial processes that occur during solid fuel combustion in a circulating fluidised bed. It combines fundamental mass balance as well as momentum equations with empirical correlations and covers 43 chemical reactions (Muskała et al., 2008; Krzywański et al., 2010a; Krzywański et al., 2010b; Krzywański et al., 2011; Krzywański et al., 2013). When fuel blend contains some amount of biomass the model needed to be modified. The previous structure was developed by including additional data from experiments carried out on the co-combustion of lignite and biomass. The model takes into account a new geometry of the system, described in Part 1 of the paper.

On the basis of solid and gas balance distributions and concentrations of solids and gaseous component profiles in the whole volume of combustion chamber were established. The modelling was performed at the same temperature and the range of the oxygen excess as in the experiment.

2.3. Hydrodynamic model

A scheme of CFB's environment established in the model is presented in Fig 4. The reaction space in the combustion chamber was divided into $N = 84$ elements, each of a height of $dH = 0.5$ m. A detailed description of the hydrodynamic model, based on the Kunii and Levenspiel correlations can be found elsewhere (Krzywański et al., 2013). The model takes into consideration two zones in the combustion chamber: a dense zone in the lower part of the combustion chamber and a dilute zone in the upper part, above the secondary air feed points. Particles pass from the dense zone to the upper dilute zone and are replaced by fresh solids.

222

Three-phase submodel of Peters (Peters, 1982) was used to describe the dense zone taking into account the existence of emulsion, bubbles and clouds in the bottom bed.

The distribution of solids concentration in the dilute zone is determined by the following equation (Kunii and Levenspiel, 1997):

$$c_v = \left(c_{v,d} - c_v^*\right)\exp\left[-a\left(z - z_d\right)\right] + c_v^* \tag{1}$$

According to the authors' suggestions c_v^* is independent of u_g and $c_v^* \leq 0.02$ for particles of group A and $c_v^* \leq 0.01$ for particles of group B, according to the classification by Geldart, whereas the constant a could be obtained from the relationships: $au_g = 2\text{-}4$ s^{-1} for Geldart A solids, 5s^{-1} for Geldart AB solids and 7s^{-1} for Geldart B solids (Kunii and Levenspiel, 1997).
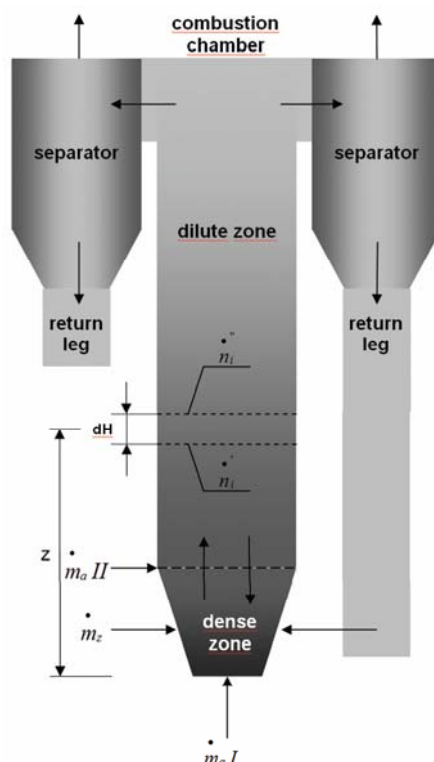

Fig. 4. Scheme of CFB's environment in the model

The hydrodynamic model enables to determine the thickness of the wall layer for a given height of the cross-sectional area in relation to the boiler grid using the Werdermann's correlation, given by Werther (2005) which was obtained on the basis of suction probe measurements in large-scale combustors.

2.4. Reaction model

The hydrodynamic parameters obtained by the above described procedure enable to carry out further calculations aimed at determination of the concentrations of gaseous components along the combustion chamber. In spite of the fact that the same devolatilisation submodel was applied the reaction model differs from the approach presented by Krzywański et al. (2013), which will be described in the next subsection. The kinetic parameters proposed by Suuberg et al. (1978) and correlations presented by Liu and Gibbs (2002) were applied to describe the composition of volatiles released from coal and biomass co-combustion, i.e. CO_2, CO, H_2, CH_4 and C_nH_m fraction in the gas, where C_nH_m was modelled as ethan C_2H_6.

Similar to the earlier work (Krzywański et al., 2013), a system of 44 chemical reactions was considered in the model. Among them are homogeneous and heterogeneous reactions including char and volatile oxidation and formation/destruction of NO and N_2O, as they were shown to be important during co-combustion process: Chen et al. (2001), Desroches-Ducarne et al. (1998), Furusawa et al. (1982), Furusawa et al. (1985), Gungor and Eskin (2008), Hayhurst and Lawrence (1996), Huilin et al. (2000), Mukadi et al. (2000), Saraiva et al. (1993), Tomeczek (1992), Tomeczek and Gardoń (2003), Tsujimura et al. (1983), Zhou et al. (2011). For the purposes of this work, substantial modifications were made including changes in chemical kinetic equations, to make them capable to consider biomass and coal co-combustion. Balance equations for the the *i*-th gaseous component in each considered cell of the combustion chamber were also used in the model (Krzywański et al., 2010). For the following elements of the combustion chamber, the substance balance of the *i*-th compound is expressed as (see also Fig. 4):

$$\dot{n}_i^{''} = \dot{n}_i^{'} + d\dot{n}_i \qquad (2)$$

where $i = 1,2,3,…p$, and *p* means a number of substances considered in the model, $p = 21$,

$$\dot{n}_i^{''} = u_g^{''} F_a C_i^{''} \qquad (3)$$

$$\dot{n}_i^{'} = u_g^{'} F_a C_i^{'} \qquad (4)$$

The change of *i*-th gas component flux can be written as:

$$d\dot{n}_i = dF_k \sum_{p_s} \dot{R}_{k_{p_s}} + \left(1-c_v\right) F_a \, dH \sum_{p_g} \dot{R}_{k_{p_g}} + \frac{dH}{H_v} \dot{n}_i^{v} \qquad (5)$$

The above equation is the sum of three terms. The first and the second terms consider changes of i-th gaseous component flux associated with heterogeneous and homogeneous reactions, respectively. The last term describes changes of i-th gaseous component flux during fuel devolatilization.

The bed temperature profile, for which calculations were made differed from the measured one within 5%.

All calculations were performed for 100% load. The system of balance differential equations was solved by the Runge-Kutta method of the 4th order using C++ language.

3. RESULTS AND DISCUSSION

To perform some preliminary model research, previously established coal mono-combustion model was used for the study of lignite and biomass co–combustion. In order to check the developed model, changes in reaction rates for 9 selected reactions were studied (Huilin et al., 2000; Liu and Gibbs, 2002; Saraiva et al., 1993).

The other 35 reactions previously incorporated into the model, including char oxidation and gasification reactions, are still taken into account as they make the model more complete. As the fuel is mainly composed of lignite the kinetic parameters for the 35 reactions remained unchanged (Krzywański et al., 2010a; Krzywański et al., 2010b; Krzywański et al., 2011). Modifications of kinetic parameters concern reactions R1–R9, listed in Table 1.

Reactions R1 and R2 describe CO and H_2 combustion and the rate expression equations for these two reactions are given in Liu and Gibbs (2002). Reactions R3 and R4 and R5 lead to NO reduction (Chen et al., 2001; Liu and Gibbs, 2002; Tsujimura et al., 1983), whereas the reactions R3 and R4 are considered to be the most important reactions of NO reduction, because of their significant impact on

NO emissions (Chen et al., 2001; Gungor and Eskin, 2008; Hayhurst and Lawrence, 1996; Liu and Gibbs, 2002; Mukadi et al., 2000). Reactions R6, R7, R8 are also applied in the set of chemical reactions as HCN is a part of fuel-N. Reaction R9 considers SO_2 reduction produced during oxidation of sulphur compounds in the fuel, similar to Huilin et al. (2000) and Saraiva et al. (1993). In reaction R9 SO_2 is reduced by calcium oxide particles, generated by the calcination of limestone.

Table 1. Reaction network for the modelling of gaseous pollutant emissions from biomass and lignite co-combustion

No.	Reaction
R1	$CO + \frac{1}{2}O_2 \rightarrow CO_2$
R2	$2H_2 + O_2 \rightarrow 2H_2O$
R3	$NO + CO \rightarrow \frac{1}{2}N_2 + CO_2$
R4	$C + NO \rightarrow \frac{1}{2}N_2 + CO$
R5	$NO + H_2 \rightarrow \frac{1}{2}N_2 + H_2O$
R6	$HCN + \frac{1}{2}O_2 \rightarrow NCO + H$
R7	$NCO + NO \rightarrow N_2O + CO$
R8	$NCO + \frac{1}{2}O_2 \rightarrow NO + CO$
R9	$SO_2 + CaO + \frac{1}{2}O_2 \rightarrow CaSO_4$

First of all the present authors applied activation energy *E* of fuel blends used during the tests, considered in this study for reactions R1 – R9. The values of activation energies of fuels taken into account can be found in Krzywański et al. (2013). Consequently, chemical reaction rate coefficients for 9 chemical reactions had to be also modified. The rates for chemical reactions R1 – R8 were determined using solid dependence - type equations:

$$k_i = A_i C_v^{m_{1i}} T^{m_{2i}} \exp\left[-\left(E/RT\right) + E_{0i}\right] \tag{6}$$

while the rate of reaction R9 was described similarly as by others (Knobig et al., 1998; McIlven-Wright et al., 2006) with modifications presented later in the paper.

Kinetic parameters of nine chemical reactions were obtained numerically and they are listed in Table 2. They take into consideration the properties of fuels and limestone including activation energy, volatile and sulfur content of fuel blends, biomass share, and limestone reactivity.

The other 35 reactions have been applied in the model making it more complete. The kinetic parameters for these reactions remained unchanged, since the fuel mainly constituted of lignite (Krzywański et al., 2010a; Krzywański et al., 2010b; Krzywański et al., 2011).

Chemical reaction rate coefficients defined in this way allowed to achieve good agreement between experimentally obtained and calculated gaseous pollutant emissions.

Table 2. Reaction rate expressions and rate coefficients for reactions R1-R9

No	Rate expression	A	m_1	m_2	E_0
R1	$k_1 C_{co} C_{H_2O}^{0.5} O_2^{0.5}$	$3.25 \cdot 10^{-7}(-2.99u_b + 1.45)\exp(1.17 \cdot 10^{-4} E)$	1.62	-8.17	-90.24
R2	$k_2 C_{H_2}^{1.5} O_2$	$1 \cdot 10^{12}$	1.08	4.45	-18.46
R3	$k_3 C_{NO}$	$1.01 \cdot 10^4 \exp(41.83u_b)$	0.90	10.50	-71.63
R4	$k_4 C_{NO}$	1	$-2.6u_b + 0.97$	-2.06	20.92
R5	$k_5 C_{H_2} C_{NO}$	1	-0.03	3.24	-5.25
R6	$k_6 C_{O_2} C_{HCN}$	1	0.42	-4.44	46.83
R7	$k_7 C_{O_2} C_{HCN} C_{NO}$	1	-1.46	0.11	-2.32
R8	$k_8 C_{O_1} C_{HCN} C_{NO}$	1	2.67	0.26	26.76
R9	$k_9 C_{SO_1}$	$k_9 = (\pi/6) \cdot d_s^3 F_s L_s k_0 \exp(-E/RT)$ $k_0 = 1.862 \cdot 10^{20} u_b - 1.736 \cdot 10^{21} S_{tot} - 1.264 \cdot 10^{20} \cdot VM_{tot} + 3.015 \cdot 10^{19}$ $F_s = -38.4 T + 5.6 \cdot 10^4 \quad T \geq 1253K$ $F_s = 35.9 T + 3.67 \cdot 10^4 \quad T < 1253K$ (Huilin et al., 2000; Saraiva et al., 1993)			

A comparison between the measured and predicted CO_2, CO, SO_2 and NO_x emissions is shown in Fig. 5.
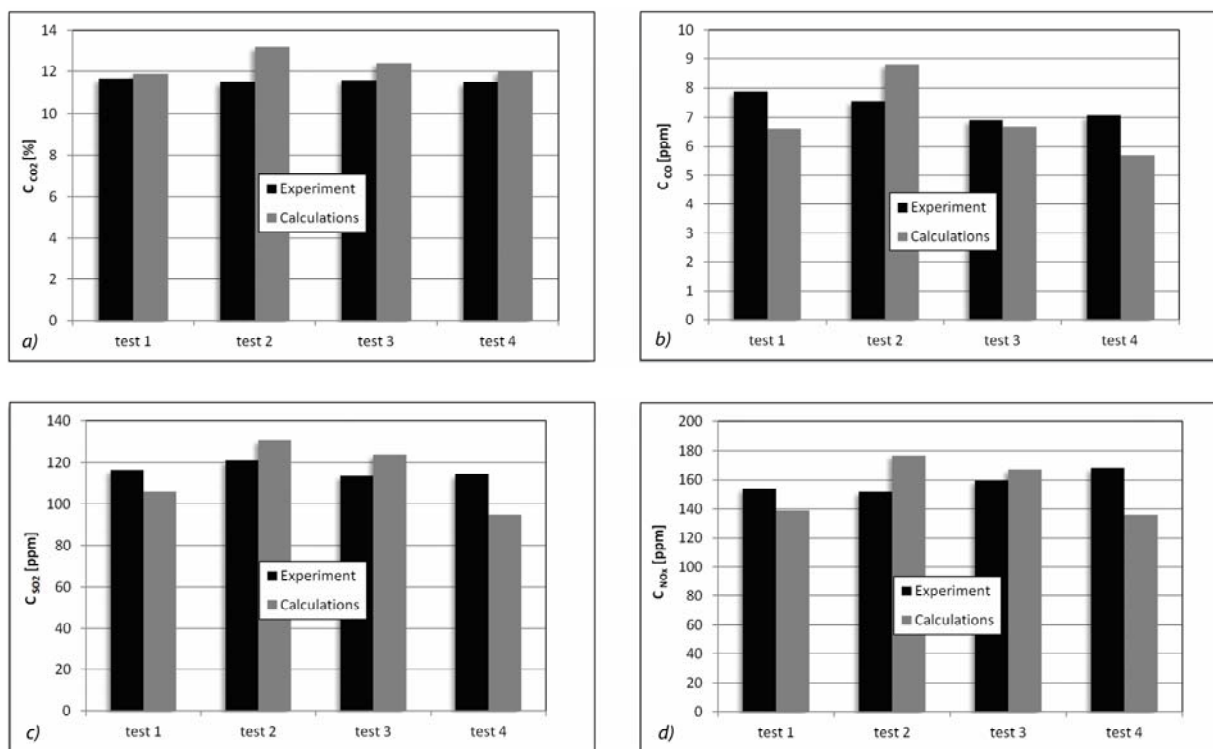

Fig. 5. Comparison of : a) CO_2, b) CO, c) SO_2 and d) NO_x experimental and calculated concentrations in dry flue gas

As can be seen, the data obtained from calculation are located within the range of ± 20%. Some under- and overestimation of gaseous flue gas component emissions can be attributed to the assumed hydrodynamics of the sub-model, averaging the concentration profiles of the bed material. There is an indication that more experimental data are needed in order to validate the model parameters.

In order to determine the impact of the 9 reactions on CO_2, CO, SO_2 and NO_x emissions a sensitivity analysis was carried out.

The analysis consisted in calculating the ratios $C_{CO_2 Hi} C_{CO_2 calc}^{-1}$, $C_{CO Hi} C_{CO calc}^{-1}$, $C_{SO_2 Hi} C_{SO_2 calc}^{-1}$, $C_{NO_x Hi} C_{NO_x calc}^{-1}$, where the subscript *Hi* corresponds to the gas component emission predicted with the particular reaction rate increased to 10 times of its previous value. The analysis was performed for tests 1 and 4.

The procedure was similar to the method described by Liu and Gibbs (2002). The closer to one the values of the ratio tend to be, the lesser effect the reaction has on a flue gas component emission.

It was observed in the CO_2 case, where ratios for all the reactions are nearly equal to 1 (Fig. 6a). Some deviations from unity, e.g. for R1 and R2 take the values in the range of 0.996 to 1.005, so they are negligibly small. The results are consistent with the conclusions of McIlven-Wright (2006) that generally co-firing has an almost negligible effect on CO_2 emissions.
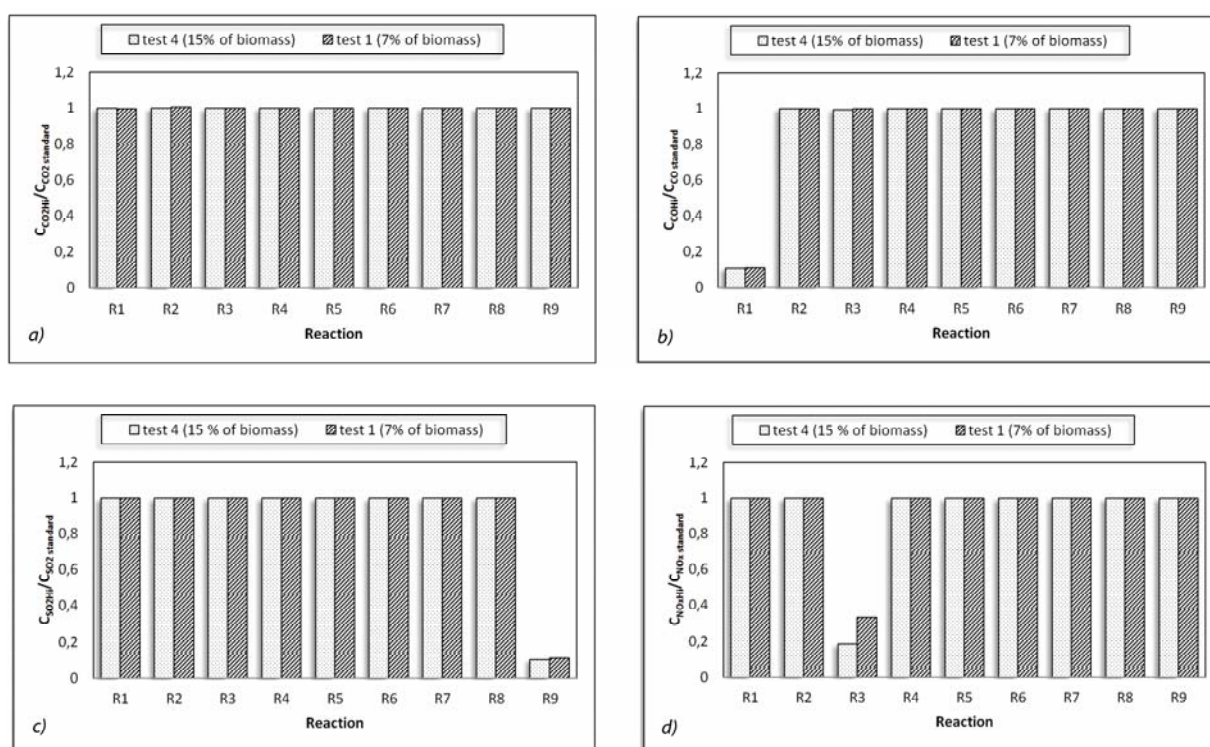

Fig. 6. The effect of individual reaction rate, multiplied by 10 on: a) CO_2, b) CO, c) SO_2 and d) NO_x emissions for tests 1 and 4

Fig. 6b shows that the reaction R1 has a great influence while the others, especially R3 and R4, have a negligibly small effect on CO emissions.

Only the reaction R9 affects the emissions of SO_2, which is obvious (Fig. 6c). Among all nine considered reaction only the reaction R3 plays an important role in NO_x emissions (Fig. 6d). The ratios

$C_{NO_xHi} C^{-1}_{NO_{x,calc}}$ resulting from other reactions, especially for the reaction R4 are close to 1. The obtained results confirm the opinion that the reaction R3 belongs to the most important reactions affecting NO emission (Chen et al., 2001; Gungor and Eski, 2008; Hayhurst and Lawrence, 1996; Liu and Gibbs, 2002; Mukadi et al., 2000). Such a behavior could be explained by the total carbon content in the fuel blend used in the study. As fuel blends mainly constituted of lignite with a low carbon content (in the range of 27%–29.3%) a relatively small addition of biomass with a significantly higher carbon content of 47.13% – 48.6% (Krzywański et al., 2013) yields the total carbon content in the fuel blends in the range of 28%–30%. It seems to be still sufficient amount of carbon in the fuel to allow the R3 reaction between CO and NO to play a major role in NO_x reduction mechanism. The important impact of CO in the NO reduction mechanism is also emphasised by Chen et al. (2001). The authors remarked that the reaction of CO with NO on char could be considered as a part of the heterogeneous reaction R4 occurring in the presence of CO.

It could be seen from Fig. 6d that the NO_x concentration is lower in test 4 than that in test 1. It could be a result of about 1% higher carbon content in the fuel blend during the test 4 than in the test 1, as the fuel blend applied in the test 4 contains more than twice of the amount of biomass as compared to test 1. It is also consistent with the literature (Armesto et al., 2003) that a slight decrease of NO_x emissions was noticed during co-combustion due to higher volatile matter content in biomass.

4. CONCLUSIONS

The emissions of CO, SO_2 and NO_x from lignite and biomass co-combustion in a large – scale large-scale 261 MWe COMPACT circulating fluidised bed boiler are discussed in the paper. The following conclusions can be drawn:

- Carbon monoxide content in the flue gas decreases with the biomass share for all types of biomass used in this work due to the nature of volatile combustion, which takes place in the upper part of the combustion chamber, enhancing burnout there.
- SO_2 emissions decreased with the biofuel fraction, due to a lower S content for all types of biomass than that in lignite.
- Lower NO_x emissions were also observed for all types of biomass as compared to lignite, mainly due to higher char content in the biofuels.

A computational model applied to calculate CO_2, CO, SO_2 and NO_x emissions during biomass and lignite co-combustion in a circulating fluidised bed boiler was also proposed. The model covers formation of different gaseous pollutants and their destruction paths.

The obtained results (simulated data) are located within the range ± 20% for CO and NO_x, and ± 15% for CO_2 and SO_2 when compared with experimental results.

A comparison of the experimental and computational data points to the need of modifying the existing formulas for the rate constant coefficients for the formation and destruction of gaseous pollutant emission reactions that occur during co-combustion of lignite and biomass.

The authors proposed equations for the chemical reaction rate coefficients of eight reactions which were used to describe biomass and lignite co-combustion in CFB conditions.

SYMBOLS

A	constant
C	gas concentration, kmol m^{-3}
c_v	volume fraction of solids,
$c_{v,d}$	volume fraction of solids in the bottom dense zone,
c_v^*	volume fraction of solids in the upper dilute zone,
dH	height of each element into which the combustion chamber was divided, m
D_e	hydraulic combustion chamber diameter, m
E	activation energy, kJ mol^{-1}
E_0	activation energy constant,
E_{0i}	constant,
F_s	surface area, m^{-1}
F_a	boiler cross-section area, m^2
F_k	external surface area of particle, m^2
L_s	limestone reactivity,
H_k	combustion chamber height, m
k	chemical reaction rate coefficient, s^{-1}
m_{1i}, m_{2i}	constants,
$\dot{m}_a$	air flux, kg s^{-1}
$\dot{m}_z$	fuel flux, kg s^{-1}
$\dot{n}_i$	i-th gas component flux, mol s^{-1}
$\dot{n}_i^v$	i-th gas component volatile matter flux, mol s^{-1}
R	universal gas constant, J mol^{-1}K^{-1}
R_k	reaction rate, kmol s^{-1}
S_{tot}	sulphur content in fuel blend,
T	bed temperature, K
u_b	share of biomass in fuel blend
u_g	gas velocity, m s^{-1}
VM_{tot}	volatile content in fuel blend,
z	distance of cross-section area from the grid, m
z_d	the height of the dense zone, m
δ_{hsp}	thickness of the wall layer, m

Subscripts

calc.	data obtained by calculations
exp.	obtained in experiment
g	data obtained by calculations

REFERENCES

Abelha P., Gulyurtlu I., Crujeira T., Cabrita I., 2008. Co-combustion of several biomass materials with bituminous coal in a circulating fluidized bed combustor. *9th International Conference on Circulating Fluidized Beds in conjunction with the 4th International VGB Workshop Operating Experience with Fluidized Bed Firing Systems*, Hamburg, Germany, 2008.

Armesto L., Bahillo A., Veijonen K., Cabanillas A., Otero J., 2002. Combustion behaviour of rice husk in a bubbling fluidised bed. *Biomass Bioenerg.*, 23, 171–179. DOI: 10.1016/S0961-9534(02)00046-6.

Armesto L., Bahillo A., Cabanillas A., Veijonen K., Otero J., Plumed A., Salvador L., 2003. Co-combustion of coal and olive oil industry residues in fluidised bed. *Fuel*, 82, 993–1000. DOI:10.1016/S0016-2361(02)00397-6.

Bahillo A., Cabanillas A., Gayan P., Diego L.D., Adanez J., 2003. Co-combustion of coal and biomass in FB boilers: model validation with experimental results from CFB pilot plant. *46th Int. Energy Agency – Fluidized Bed Conversion (IEA – FBC)*, Jacksonville, FL, USA, 2003.

Chen Z., Mu Lin, Ignowski J., Kelly B., Linjewile T.M., Agarwal P.K., 2001. Mathematical modelling of fluidized bed combustion. 4: N_2O and NO_x emissions from the combustion of char. *Fuel*, 80, 1259–1272. DOI: 10.1016/S0016-2361(01)00007-2.

Desroches-Ducarne E., Dolignier J. C., Marty E., Martin G., Delfosse L., 1998. Modelling of gaseous pollutants emissions in circulating fluidized bed combustion of municipal refuse. *Fuel*, 77, 1399–1410. DOI: 10.1016/S0016-2361(98)00060-X.

Furusawa T., Tsunoda M., Kunii D., 1982. Nitric oxide reduction by hydrogen and carbon monoxide over char surface. Fundamental kinetics for nitric oxide emission control from fluidized-bed combustor of coal, In: Wei J., Georgakis Ch. (Eds.), *Chemical Reaction Engineering – Boston. ACS Symposium Series*, 196, Chapter 29, 347–357. DOI: 10.1021/bk-1982-0196.ch029.

Furusawa T., Tsujimura M., Yasunaga K., Kojima T., 1985. Fate of fuel bond nitrogen within fluidized-bed combustor under staged air firing, *8th International Conference on Fluidized-Bed Combustion*, Houston, TX, USA, 1985.

Gayan P., Adanez J., Diego L.F., Garcia-Labiano F., Cabanillas A., Bahillo A., Aho M., Veijonen K., 2004. Circulating fluidised bed co-combustion of coal and biomass. *Fuel*, 83, 277–286. DOI: 10.1016/j.fuel.2003.08.003.

Gungor A., Eskin N., 2008. Two-dimensional coal combustion modelling of CFB. *Int. J. Therm. Sci.*, 47, 157–174. DOI: 10.1016/j.ijthermalsci.2007.01.017.

Hayhurst A.N., Lawrence A.D., 1996. The amounts of NO_x and N_2O formed ina fluidized bed combustor during the burning of coal volatiles and also of char. *Combust. Flame*, 105, 341–357. DOI: 10.1016/0010-2180(95)00215-4.

Hein K.R.G., Bemtgen J.M., 1998. EU clean coal technology—co-combustion of coal and biomass. *Fuel Process. Technol.*, 54, 159–169. DOI: 10.1016/S0378-3820(97)00067-2.

Hupa M., 2005. Interaction of fuels in co-firing in FBC. *Fuel* 84, 1312–1319. DOI: 10.1016/j.fuel.2004.07.018.

Huilin L., Guangbo Z., Rushan B., Yongjin C., Gidaspow D., 2000. A coal combustion model for circulating fluidized bed boilers. *Fuel*, 79, 165–172. DOI: 10.1016/S0016-2361(99)00139-8.

Jenkins B.M., Baxter L.L., Miles Jr. T.R., Miles T.R., 1998. Combustion properties of biomass. *Fuel Process. Technol.*, 54, 1–3. DOI: 10.1016/S0378-3820(97)00059-3.

Knobig T., Werther J., Amand L.-E., Leckner B., 1998. Comparison of large- and small-scale circulating fluidized bed combustors with respect to pollutant formation and reduction for different fuels. *Fuel*, 77, 1635–1642. DOI: 10.1016/S0016-2361(98)00092-1.

Krzywański J., Czakiert T., Muskala W., Sekret R., Nowak W., 2010a. Modelling of solid fuels combustion in oxygen-enriched atmosphere in circulating fluidized bed boiler. Part 1. The mathematical model of fuel combustion in oxygen-enriched CFB environment. *Fuel Process. Technol.*, 91, 290–295. DOI: 10.1016/j.fuproc.2009.10.011.

Krzywański J., Czakiert T., Muskala W., Sekret R., Nowak W., 2010b. Modelling of solid fuel combustion in oxygen-enriched atmosphere in circulating fluidized bed boiler. Part 2. Numerical simulations of heat transfer and gaseous pollutant emissions associated with coal combustion in O_2/CO_2 and O_2/N_2 atmospheres enriched with oxygen under circulating fluidized bed conditions. *Fuel Process. Technol.*, 91, 364–368. DOI: 10.1016/j.fuproc.2009.11.008.

Krzywański J., Czakiert T., Muskała W., Nowak W., 2011. Modelling of CO_2, CO, SO_2, O_2 and NO_x emissions from the oxy – fuel combustion in a circulating fluidized bed. *Fuel Process. Technol.*, 92, 590–596. DOI: 10.1016/j.fuproc.2010.11.015.

Krzywański J., Rajczyk R., Bednarek M., Wesolowska M., Nowak W., 2013. Gas emissions from a large scale circulating fluidized bed boilers burning lignite and biomass. *Fuel Process. Technol.*, 116, 27–34. DOI: 10.1016/j.fuproc.2013.04.021.

Krzywański J., Rajczyk R., Komorowski M., Nowak W., 2012. Model research of coal and biomass co-combustion in a large scale circulating fluidized bed boiler, *37th International Technical Conference on Clean Coal & Fuel Systems,* Clearwater, FL, USA, 2012.

Kunii D., Levenspiel O., 1997. Circulating fluidized-bed reactors. *Chem. Eng. Sci.*, 52, 2471–2482. DOI: 10.1016/S0009-2509(97)00066-3.

Leckner B., 2007. Co-combustion – A summary of technology. *Thermal Sci.*, 11, 5–40. DOI: 10.2298/TSCI0704005L.

Leckner B., 2008. The role of CFB in co-combustion. *9th International Conference on Circulating Fluidized Beds in conjunction with the 4th International VGB Workshop Operating Experience with Fluidized Bed Firing Systems*, Hamburg, Germany, 2008.

Leckner B., Amand L.-E., Lucke K., Werther J., 2004. Gaseous emissions from co-combustion of sewage sludge and coal/wood in a fluidized bed. *Fuel*, 83, 477–486. DOI: 10.1016/j.fuel.2003.08.006.

Liu H., Gibbs B.M., 2002. Modelling of NO and N_2O emissions from biomass – fired circulating fluidized bed combustors. *Fuel* 81, 271–280. DOI: 10.1016/S0016-2361(01)00170-3.

Lyngfelt A., Leckner B., 1999. Combustion of wood-chips in circulating fluidized bed boilers – NO and CO emissions as functions of temperature and air-staging. *Fuel*, 78, 1065–1072. DOI: 10.1016/S0016-2361(99)00006-X.

McIlveen-Wright D.R., Pinto F. , Armesto L., Caballero M.A., Aznar M.P., Cabanillas A., Huang Y., Franco C., Gulyurtlu I., McMullan J.T., 2006. A comparison of circulating fluidised bed combustion and gasification power plant technologies for processing mixtures of coal, biomass and plastic waste. *Fuel Process. Technol.*, 87, 793–801. DOI: 10.1016/j.fuproc.2006.04.002.

Mukadi L., Guy C., Legros R., 2000. Prediction of gas emissions in an internally circulating fluidized bed combustor for treatment of industrial solid wastes. *Fuel*, 79, 1125–1136. DOI: 10.1016/S0016-2361(99)00251-3.

Muskała W., Krzywański J., Sekret R, Nowak W., 2008. Model research of coal combustion in circulating fluidized bed boilers. *Chem. Process Eng.*, 29, 473–492.

Nussbaumer T., 2003. Combustion and co-combustion of biomass: fundamentals, technologies, and primary measures for emission reduction. *Energy Fuels*, 17, 1510–1521. DOI: 10.1021/ef030031q.

Peters M.H., Fan L.S., Sweeney T.L., 1982. Reactant dynamics in catalytic fluidized bed reactors with flow reversal of gas in the emulsion phase. *Chem. Eng. Sci.,* 37,553–565. DOI: 10.1016/0009-2509(82)80118-8.

Rajczyk R., Mirek P., Walkowiak R., Nowak W., 2011. Operational experience in the material department (PGE GiEK) of the Turow Power Plant, *VGB Powertech* 9, 90–93.

Saraiva P.C., Azvedo J.L.T., Carvalho M.G., 1993. Mathematical simulation of a circulating fluidized bed combustor. *Combust. Sci. Technol.*, 93, 223–243. DOI: 10.1080/00102209308935291.

Sami M., Annamalai K., Wooldridge M., 2001. Co-firing of coal and biomass fuel blends. *Progr. Energ. Combust.*, 27, 171–214. DOI: 10.1016/S0360-1285(00)00020-4.

Skreiberg O., Kilpinen P., Glarborg P., 2004. Ammonia chemistry below 1400 K under fuel-rich conditions in a flow reactor. *Combust. Flame* 136, 501–518. DOI: 10.1016/j.combustflame.2003.12.008.

Suuberg E.M., Peters W.A. Howard J.V., 1978. *Proc. 17 – Symp. Combustion (Int.) Combustion Institute.* 1978, Pittsburgh, USA, 117–130.

Thunman H., Leckner B., Niklasson F., Johnsson F., 2002. Combustion of wood particles — A particle model for Eulerian calculations. *Combust. Flame*, 129, 30–46. DOI: 10.1016/S0010-2180(01)00371-6.

Tomeczek J. (1992). *Spalanie węgla*. Wydawnictwo Politechniki Śląskiej Gliwice, Poland.

Tomeczek J., Gradoń B., 2003. The role of N_2O and NNH in the formation of NO via HCN in hydrocarbon flames. *Combust. Flame*, 133, 311–322. DOI: 10.1016/S0010-2180(03)00013-0.

Tsujimura M., Furusawa T., Kunii D., 1983. Catalytic reduction of nitric oxide by hydrogen over calcined limestone. *J. Chem. Eng. Jpn.*, 16, 524–526.

Werther J., 2005. Fluid dynamics, temperature and concentration fields in large – Scale CFB combustors. *8-th International Conference on Circulating Fluidized Beds*, 2005, Hangzhou, China.

Werther J., 2009. Potentials of biomass co-combustion in coal-fired boilers. *20th International Conference on Fluidized Bed Combustion*, 2009, Xi'an China.

Yu Z.S., Ma X.Q., Lai Z.Y., Xiao H.M., 2009. CFD modelling applied to the co-combustion of paper sludge and coal in a 130 t/h CFB boiler. *20th International Conference on Fluidized Bed Combustion*, 2009, Xi'an China.

Zhou W., Zhao C., Duan L., Liu D., Chen X., 2011. CFD modelling of oxy-coal combustion in circulating fluidized bed. *Int. J. Greenh. Gas Con.*, 5, 1489–1497. DOI: 10.1016/j.ijggc.2011.08.006.